Lab on a Chip

RSC Publishing

PAPER

View Article Online
View Journal | View Issue

Cite this: *Lab Chip*, 2013, **13**, 562

Adhesive micro-line periodicity determines guidance of axonal outgrowth†

Steven R. Hart,*[a] Yu Huang,[a] Thomas Fothergill,[b] Derek C. Lumbard,[b] Erik W. Dent[b] and Justin C. Williams[a]

Received 17th October 2012,
Accepted 27th November 2012

DOI: 10.1039/c2lc41166k

www.rsc.org/loc

Adhesive micro-lines of various sub-cellular geometries were created using a non-traditional micro stamping technique. This technique employed the use of commercially available diffraction gratings as the molds for the micro stamps, a method which is quick and inexpensive, and which could easily be adopted as a patterning tool in a variety of research efforts. The atypical saw-tooth profile of the micro stamps enabled a unique degree of control and flexibility over patterned line and gap widths. Cortical neurons cultured on patterned poly-lysine micro-lines on PDMS exhibit a startling transition in axonal guidance: From the expected parallel guidance to an unexpected perpendicular guidance that becomes dominant as patterned lines and gaps become sufficiently narrow. This transition is most obvious when the lines are narrow relative to gaps, while the periodicity of the pattern is reduced. Axons growing perpendicular to micro-lines exhibited 'vinculated' growth, a unique morphological phenotype consisting of periodic orthogonal extensions along the axon.

Introduction

The ability to guide and direct the growth of axons with engineered precision is an on-going endeavor with broad implications for many diverse areas of research. These include implantable devices for nervous system injury recovery,[1] the study of neurological disorders and diseases,[2] efforts to create well-defined neural networks,[3,4] as well as basic neuroscience investigations, such as signal transduction[5] and growth cone biomechanics.[6] While many efforts at the interface of engineering and neuroscience have yielded encouraging results, many avenues, including even the very accessible, have been left unexplored.

Surface patterning to direct cellular behavior is achieved through a variety of methods.[7] When patterning parallel lines to study neuron outgrowth, however, one of two motivations usually dictates the design parameters. For patterning ease, commonly both the patterned lines and gaps are relatively wide,[8,9] or for cell isolation, relatively narrow lines are separated by large gaps.[10] While axonal guidance response on typically patterned micro-lines is relatively well characterized, guidance on parallel patterned lines and gaps of small, sub-cellular dimensions is not. To understand the cause of this knowledge deficit, consideration of the following aspects of micropattern creation is useful: To create patterns over a 'large' area (>1 mm^2), a useful size for studying statistically relevant sample sizes, relatively inexpensive methods such as micro-stamping (or micro-contact printing) are typically employed. But to create a microstamp with single-micron scale features requires an expensive mask. Moreover, if the desired features are parallel lines with equally small gaps, defects[11] may become too overwhelming to make this approach attractive. On the other hand, patterning at fairly high ($\sim$1 μm) resolution has been accomplished by a variety of alternative techniques. However, these techniques are generally not well suited to pattern over a large area and require specialized and costly equipment and training. To create a large-scale pattern of parallel lines would be tedious. Moreover, the intuitive, widely-accepted paradigm of neuronal line guidance is that if patterned lines are spaced too closely, growth will simply become increasingly random.[12]

In this work, a non-traditional method of micro-stamping was employed. Commercially available diffraction gratings were used in lieu of a standard silicon master to create micro stamps. Although using stamps from diffraction gratings to create micropatterns has been previously accomplished,[13] such patterns have not been employed for cellular research generally, or for neural patterning specifically. These micro-line stamps have several advantages relative to traditional micro-stamps. They are very inexpensive and require only very simple fabrication techniques, and simultaneously grant access to single-micron resolution patterning. Although traditional micro-stamping is already viewed as reasonably accessible, the method presented here is exceedingly more so. Also, unlike many other high-resolution patterning schemes, this

[a]*University of Wisconsin-Madison – Biomedical Engineering, Madison, Wisconsin, USA. E-mail: srhart2@wisc.edu*

[b]*University of Wisconsin-Madison – Neuroscience, Madison, Wisconsin, USA*

† Electronic supplementary information (ESI) available. See DOI: 10.1039/c2lc41166k

technique requires no expensive equipment and can be very easily adopted without specialized training. In spite of intrinsic pattern limitations due to commercial availability and design, this approach of micro-line stamping could easily be adopted by biology-based labs to perform a wide variety of experiments. Indeed, this study will show that neurons cultured on these micro-lines display extremely diverse modes of guidance, dependent primarily on the geometry of the underlying pattern. It is as of yet unclear whether there is a strong *in vivo* corollary for the results presented here. What is clear, though, is that the axon outgrowth behavior is non-intuitive and would be difficult or impossible to predict *in vivo* without the *in vitro* results made possible by this micro-line methodology.

Another interesting facet is that these stamps have an atypical surface profile (saw tooth *vs.* traditional rectangular). Thus, the stamped line width is easily tunable, a possibility previously conceived[14] and demonstrated,[15] yet heretofore unexploited in any biological experiment. Compared with the burdensome process of designing a line assay or other experiments with easily varied line widths using traditional micro stamps, this approach is quick and efficient. The scale of patterning is also of particular interest, given the large body of work devoted to neurite guidance on topographic features of similar scale in the lateral dimensions.[16–18]

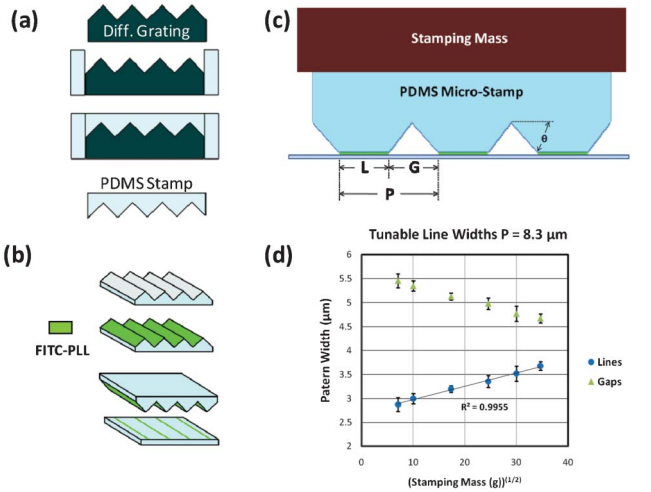

Fig. 1 Stamp Fabrication and Characterization (a) PDMS micro-stamps are molded off of a commercially-available diffraction grating. (b) PDMS stamps are inked with FITC-PLL, inverted and stamped onto surface (PDMS) with controlled force. (c) As stamping mass is increased, thus compressing the PDMS stamp, patterned line width (L) becomes larger and the gap width (G) becomes smaller in a codependent relationship with the periodicity (P) (L + G = P). θ is the blaze angle. (d) Increasing stamping force yields patterned lines (or gaps) of greater (lesser) width in a predictable manner. The line width scales with the mass (or equivalently, force) raised to the ½ power. Error bars: ± standard error (SE).

Materials and methods

PDMS micro-stamp and culture substrate creation

Reflective ruled diffraction gratings were bought commercially (Optometrics). Diffraction gratings are characterized by two measurements: grooves per millimeter (g mm^{-1}) and blaze angle (θ) (Fig. 1c). The blaze angle determines the degree of asymmetry of the surface profile, with a 45° angle being perfectly symmetric. In this study gratings with dimensions of 120 g mm^{-1} (θ = 46° 3′), 150 g mm^{-1} (θ = 35°), 300 g mm^{-1} (θ = 36° 52′), and 600 g mm^{-1} (θ = 28° 41′) were used. These correspond to a line periodicity of 8.3 μm, 6.7 μm, 3.3 μm, and 1.7 μm, respectively. All gratings (and stamps) have surface area dimensions of 12.75 mm × 12.75 mm. Gratings were inserted into a custom made polydimethylsiloxane (PDMS) mold. PDMS (184 Sylgard – Dow Corning) was mixed in a 10 : 1 ratio (base: curing agent), poured into the mold, and baked on a covered hot plate for 30 min. at 85 °C. The newly formed PDMS stamp was cut out and stored until inking, while the grating could be reused indefinitely. For the culture substrates, uncured PDMS (10 : 1) was poured into a 100 mm petri dish, allowed to settle until flat, and baked for 30 min. at 85 °C. 2 cm × 2 cm squares were cut out of the cured thick film (~0.5 mm) and autoclaved for 1 h at 120 °C.

Inking and stamping

PDMS micro-stamps were covered in FITC labeled poly-L-lysine (30–70 kDa, P3069 Sigma-Aldrich) at a 1 mg ml^{-1} concentration for 1 h, after which the surface was twice washed with sterile, distilled, deionized water. This process was repeated 3 times, after which the stamps were allowed 30 min to dry. Immediately prior to stamping and after autoclaving, the PDMS culture substrate was briefly (20 s) air-plasma treated using a plasma wand (ETP Model BD-20) to enhance FITC-PLL transfer. The pattern transfer was performed by inverting the stamp, setting it on the PDMS substrate, and applying force orthogonal to the surface. To achieve calibration of narrow lines, masses from 50 g to 1200 g were placed upon the stamp. Wider lines (uncharacterized) were achieved by larger forces, applied directly by hand. After the force was applied for 60 s. the stamp was lifted off, and the substrate kept in a darkened location until culturing.

Line width characterization

Micro-lines were imaged fluorescently using a 20× objective on an inverted microscope, with images captured in MetaMorph. Line profiles were taken using Image J software, averaged over at least 30 μm. The edge of the line was defined as a 20% increase in fluorescent intensity from the background level. Characterizations were performed by performing at least 4 independent stamping tests for each stamp dimension. Each test consisted of a minimum of 20 line width measurements from 4 different locations on the stamped surface. To measure the line width on substrates used for culture, at least 20 measurements were made from 4 different locations and averaged.

Neuron cell culture and immunostaining

All mouse procedures were approved by the University of Wisconsin Committee on Animal Care and were in accordance with NIH guidelines. Neurons used in this study were E15.5 cortical neurons from Swiss Webster mice. Cells were isolated

and cultured according to established methods.[19] Briefly, cells were dissociated by treating with trypsin (0.25%, 15 min, 37 C), triturated with a micropipette tip, and diluted in plating medium (neurobasal medium with 5% FBS, Hyclone, B27 supplement, 2 mM glutamine, 37.5 mM NaCl, and 0.3% glucose). Cells were plated onto PDMS substrates at a density of 6000 cells cm^{-2}. One hour later, the sample is flooded with serum-free medium (plating medium without FBS) and incubated for 48 h. Neurons were fixed in 4% PKS[20] (PFA/Krebs Solution) at 37 C for 15 min to retain cytoskeletal integrity, before being washed three times with PBS. Cells that are to be immuno-stained were permeabilized for 10 min in 0.2% Triton X-100 then washed once with 1% BSA/PBS before blocking in 10% BSA/PBS for an hour. Anti-tyrosinated tubulin antibodies (Millipore) were used to label dynamic microtubules and actin filaments were revealed using Alexa-647 labeled Phalloidin (Invitrogen).

Imaging and data analysis

Non-stained cells were imaged with a 20× phase objective inverted microscope, captured with Metamorph software. For each sample 80–100 cells were imaged. For each given condition, 4–6 independent samples were analyzed. Although cells in close proximity to other cells displayed consistent outgrowth behavior, cells were chosen that were relatively isolated for clarity. The outgrowth direction was determined by the angle between the micropattern and a line from the tip of the axon to the soma. All angular measurements were made using Image J software. Statistical analysis as follows: Axons growing in a given direction were grouped in 10° bins, and the relative percentages in each bin and across micro-line geometries were compared by Single Factor ANOVA. Stained cells were imaged at 100× in DIC and widefield using a Nikon TE2000 inverted fluorescence microscope and manipulated using Metamorph software. TIRF microscopy was used for imaging FITC-labeled PDL lines to increase contrast. Overlaid images were created using Image J. In images that include the label for actin filaments (blue), a despeckling processing was used to enhance the image.

Results

PDMS stamp characterization

The periodicity of printed lines was varied by molding polydimethylsiloxane (PDMS) stamps off of diffraction gratings of different geometries (Fig. 1). PDMS stamps were molded off of these gratings, inked with poly-lysine and stamped onto a smooth PDMS surface. A greater range of periodicity is possible, but beyond the scope of the present study.

All experiments used a PDMS surface stamped with poly-lysine micro-lines. Along with traits of biocompatibility and optical transparence, PDMS is attractive for its potential biomechanical adaptability, including control over surface topography,[21] substrate elasticity,[22] and surface hydrophobicity.[23] Moreover, an uncoated PDMS substrate offers a relatively non-permissive background to growing neurons, a feature which is desirable in micro-pattern stamping for neuronal guidance.[24]

A very distinctive feature of micro line stamps cast from diffraction gratings is the ability to tune the patterned line widths by varying the stamping force, a feature which arises from the saw-tooth profile of the diffraction gratings. Line width was controlled by varying the force on the microstamp during the pattern transfer (Fig. 1c). Larger forces cause an increase of line width (L) and a decrease in gap width (G), as determined by the periodicity (P) (L + G = P). Characterizations were performed using the stamp with P = 8.3 μm. These stamps also benefited from being nearly perfectly symmetric (θ = 46° 3′). On PDMS surfaces, line widths from 2.9 μm to 3.7 μm were obtained by using a stamping mass from 50 g to 1200 g (Fig. 1d.). Line widths from 3.7 μm up to 6.4 μm were also obtained, though by hand as the mass placement method became impractical beyond the characterized range. Line widths from 2.2 μm to 4.8 μm and 1.7 μm to 2.3 μm were obtained with the 6.7 μm and 3.3 μm periodicity stamps, respectively. All successful stamping attempts with the 1.7 μm periodicity stamp yielded a line width of 0.9 ± 1 μm.

Axonal guidance on poly-lysine micro-lines

Cortical neurons were cultured on the poly-lysine micro-lines and their outgrowth direction measured after 48 h. Angle of outgrowth is defined as the angle between the micro-lines and a straight line drawn from the soma to the tip of the presumptive axon. The presumptive axon was morphologically identified as a neurite that was at least twice the length of the next longest neurite, and at least 50 m in length. If the axon exhibited branching, only the most distal tip was considered. The neurons exhibited excellent outgrowth on the patterned PDMS surface, with the majority of the cells developing presumptive axons. Although outgrowth direction was generally well established by 48 h (2DIV), many of the cells were viable for longer periods – up to 7 DIV (data not shown).

Axonal guidance on micro-lines with constant L, varying G. In the first set of experiments L (line width) was held relatively constant, while G (gap width) was varied, by means of varying P (periodicity). L was maintained at 2.55 ± 0.25 μm while values of G = 5.5 μm, 4.4 μm, and 1.1 μm, were obtained by stamps of P = 8.3 μm, 6.7 μm, and 3.3 μm, respectively (Fig. 2a). For relatively large G, guidance was dominantly parallel to the lines. Although the growing axons showed the ability to explore the uncoated PDMS surface, they were commonly found to extend along a single line for hundreds of microns. The axonal alignment to the lines is not entirely unexpected. Interesting, though, was the prominence of a subpopulation of axons whose guidance is localized about a perpendicular orientation to the patterned lines. In decreasing G to 4.4 μm, the dominant guidance is still parallel, though less so than with larger G. The perpendicular guidance, however, is even more prevalent (Fig. 2b, d) , with 36% of presumptive axons growing within 20° of the perpendicular orientation. (With random outgrowth one would expect ~22%.) When decreasing G to 1.1 μm, the growth becomes significantly more randomized, in line with intuitive expectations for G → 0. However, far more axons grow within 20° of perpendicular (39%) than parallel (18%) to the lines. The

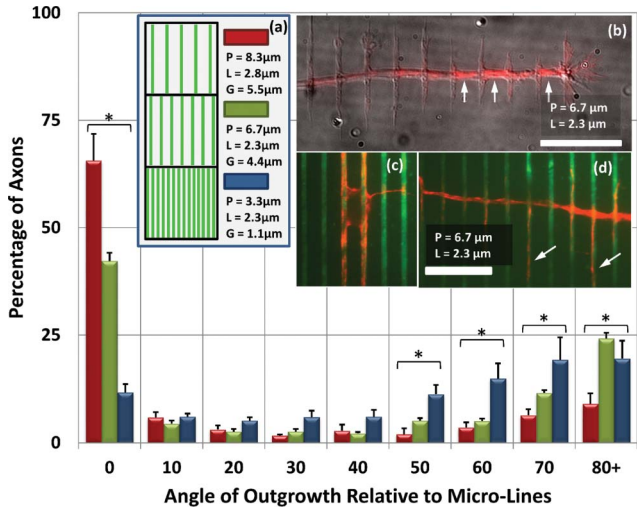

Fig. 2 Axonal Orientation on Micro-Lines of Constant L, Varying G (a) Micro-line patterns of constant line width (L = 2.55 ± 0.25 μm) are created with a variety of periodicities (P), resulting in a varied gap width (G). These data show axonal outgrowth direction on PLL patterned micro-lines on PDMS. The outgrowth angle is defined as an angle between micropatterns and a straight line drawn from the soma to the axon tip. The axonal orientation is dominantly parallel for larger values of P. However, as P is decreased, perpendicular guidance is also observed. Error bars: ± SE. Outgrowth directions marked with * indicate $p < 0.01$ for different values of P by single-factor ANOVA. (b) Perpendicular axonal outgrowth as seen on a P = 6.7 μm substrate. The image shows α-tubulin (red) overlaid on a DIC image (grey) (scale bar = 20 μm). Although a plurality of axons on this geometry grow parallel to the pattern with high fidelity, several axons turn in a perpendicular direction to the pattern. Along the perpendicular axonal shaft, several periodic extensions are growing on and parallel to the pattern, a hallmark of 'vinculated' growth. Interestingly, microtubules appear to be more concentrated in the gaps between lines (arrows). (c) The soma of a neuron with outgrowth oriented parallel to the micro-lines (green: FITC-PLL). (d) When perpendicular vinculated outgrowth is observed on the P = 6.7 μm micro-lines, frequently microtubules are seen invading orthogonal extensions (arrows). Scale bar (c) and (d): 20 μm.

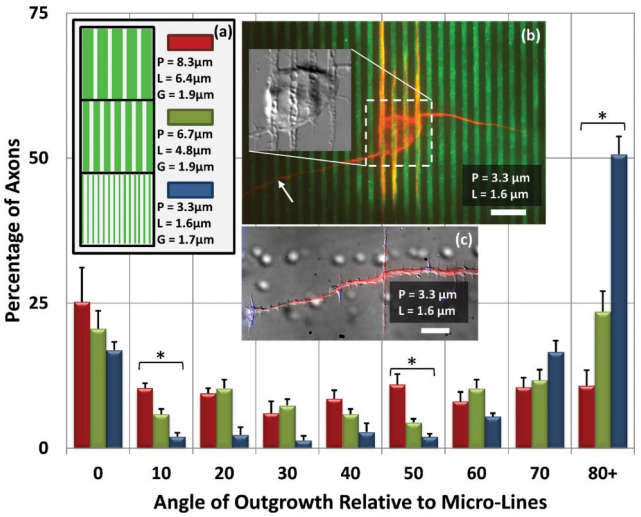

Fig. 3 Axonal Orientation on Micro-Lines of Constant G, Varying L (a) In these data, L is varied by applying differential force across the range of P such that G is now held constant (G = 1.80 ± 0.15 μm). For P = 3.3 μm, L is the minimum dimension achievable. For P = 8.3 μm, axonal growth is generally parallel to the lines, though outgrowth direction is becoming nearly randomized. And similar to Fig. 2, as P is decreased, perpendicular outgrowth increases. When P = 3.3 m, the axon outgrowth is strongly oriented perpendicular to the micro-lines. * indicates $p < 0.01$ by ANOVA. Error bars: ± SE (b) Neuron on P = 3.3 μm pattern. Arrow indicates the axon. Other neurites (presumed dendrites) mostly prefer to grow along the micro-lines. Note also the increased microtubule presence along the micro-lines in the intra-somatic region. Inset: DIC image of soma reveals an alignment of cellular structure with the micro-lines. (c) An axon on a P = 3.3 m pattern reveals vinculated growth along the axon labeled for actin filaments (blue: phalloidin, red: α-tubulin). Scale bar: 10 μm.

decrease in parallel guidance can reasonably be understood, as single growth cones are able to contact more than one line simultaneously, allowing for dispersion in growth direction. However, the increase in perpendicular guidance with decreasing gap width is anticipated to result from a unique, independent guidance mechanism.

Axonal guidance on micro-lines with constant G, varying L. In the next set of experiments, the result of changing L was examined (Fig. 3). Now G was maintained at 1.8 ± 0.2 μm, while values of L = 6.4 μm, 4.8 μm and 1.7 μm were obtained by stamps of P = 8.3 μm, 6.7 μm, and 3.3 μm, respectively. On the widest lines, axonal growth was fairly random, though more often parallel than other directions. As the line width decreases, and especially when the line width is comparable to the gap width (L = 1.7 μm, G = 1.6 μm), perpendicular orientation becomes dominant. Moreover, this perpendicular guidance is much stronger than it was for the same P with larger L (or smaller G), as in Fig. 2.

Axonal guidance on micro-lines with constant L/P (or L/G). A common element to the various results thus shown is that increasingly narrow micro-lines or gaps alone do not induce random guidance. Rather, it is when L is large relative to P that random guidance is produced. In fact, there exists a threshold L/P value above which growth increasingly becomes more random, and below which growth is strongly guided ($\pm 10^\circ$ of given orientation), seemingly independent of L/P (Fig. 4). This threshold is seen fairly clearly for P = 8.3 μm and P = 6.7 μm at L/P = 0.5. Neurons on lines of these dimensions prefer to grow parallel to the lines. It is also consistent with the results seen for P = 3.3 μm, although in this case the preferred orientation is perpendicular. Strong guidance in the preferred direction asymptotes when $L/P \leqslant 0.5$, but as L/P grows, the guidance becomes increasingly lessened, until it is entirely random by L/P = 0.7–0.8. For this reason, it is sensible to look at the guidance results when L/P is held constant. This has the additional benefit of keeping the areal density of poly-lysine coverage constant. When L/P is held at 0.5 (L/G = 1), there is a clear transition from dominant parallel guidance at P = 8.3 μm, to dominant perpendicular guidance at P = 1.7 μm (Fig. 5, 6). It is interesting that at P = 1.7 μm, parallel guidance seems to entirely vanish. It can also be seen that where it occurs, parallel growth has a very tight distribution. Indeed, growing axons were often observed to have followed a single micro-line for hundreds of microns. In contrast, the perpendicular guidance has a much wider angular distribution.

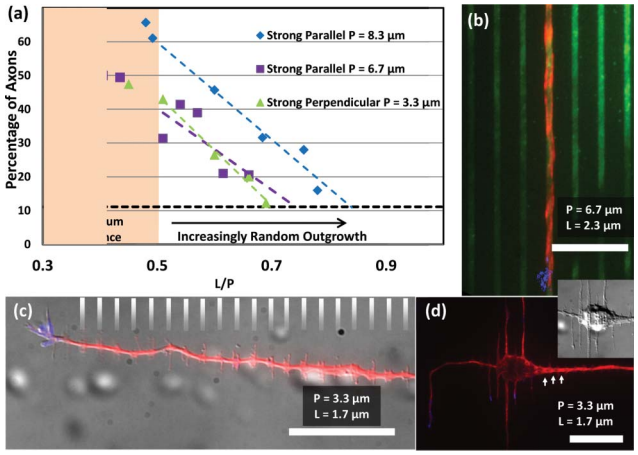

Fig. 4 Axonal Guidance Fidelity: Investigating L/P (a) Strongly guided axonal outgrowth is prevalent when L/P is small, that is, when line widths are small relative to the periodicity, largely independent of the actual value of P. However, as L/P increases above a value of 0.5, dominantly parallel (P = 8.3, 6.7 μm) or perpendicular (P = 3.3 μm) outgrowth decreases. The percentage of axons experiencing strong guidance approaches a level expected by random outgrowth (horizontal dashed line at 11%). Strong parallel guidance is defined as an outgrowth angle from 0°–10° (strong perpendicular: 80°–90°) relative to the micro-lines. (b) When L/P is small on P = 6.7 μm micro-lines, the likelihood of strongly parallel outgrowth is maximized. (c - d) For small L/P on P = 3.3 μm, strong perpendicular outgrowth is maximized. Vinculated growth, predominant dendritic alignment to the micro-lines, intra-somatic microtubule alignment, and increased microtubule density at gaps (arrows) are all evident in these images. The gray hash lines in (c) indicate the location of the micro-lines. All scale bars: 20 μm.

Vinculated growth and immuno-staining

So called 'vinculated' growth was exhibited by axons growing perpendicular to the micro-lines. This phenotype is characterized by small, filopodia-like extensions along the axonal shaft. These may occur at every location where the axon crosses a micro-line, extending up to 30 μm (Fig. 2b, 3c, 4c, 6c). Vinculated growth is observed for any value of P, regardless of whether perpendicular guidance is preferred.

To begin to discern the underlying mechanism of this type of growth we fixed and labeled neurons with an antibody to tubulin to label microtubules. When the orthogonal filopodia are longer than 20 μm (Fig. 2d, 3c), we found that microtubules had invaded the orthogonal growth, which is oftentimes coincident with stabilization of branches.[25] Also, an increased concentration of microtubules was observed in the main axonal shaft at the gaps between micro-lines (Fig. 2b, 4d). Growth of axons or dendrites parallel to micro-lines exhibits none of these effects (Fig. 2c, 3b, 4b).

In examining microtubules, the somatic region is also of interest. Microtubules are observed, even within the soma, to align themselves with the micro-lines (Fig. 3b, 4d, 6d). This is seen especially on the P = 3.3 μm, and the P = 1.7 μm substrates. For larger P, the cell body would frequently be found in between two adjacent micro-lines (Fig. 2c). Microtubules aligned along the edges of the somatic region would then typically extend into neurites growing parallel to the lines. Short neurites, constituting the presumptive

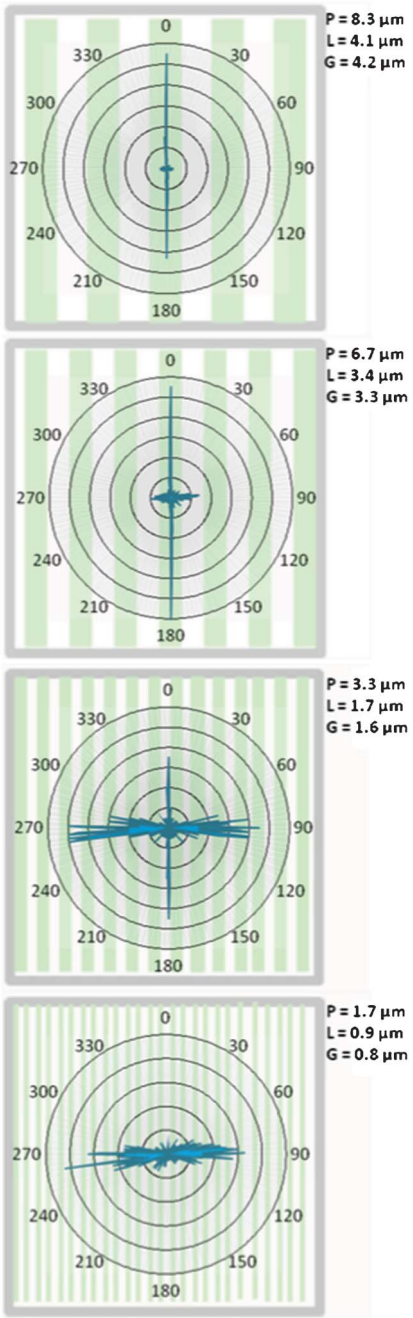

Fig. 5 Polar Distribution of Axonal Outgrowth: Varying P, Fixed L/P Axonal outgrowth direction observed when varying P while holding L/P fixed (L/P = 0.5, or equivalently, L/G = 1). In addition to values of P seen previously, P = 1.7 μm is now also included. Angles are indicated around each plot. Data are grouped in 1° bins, where the length of a line indicates the relative number of axons for a given direction, normalized for each value of P. All data are overlaid upon representative micropatterns. For each pattern dimension, n ⩾ 509 (number of counted axons) obtained from at least six independent samples. Guidance dramatically varies from predominantly parallel (P = 8.3 μm) to perpendicular (P = 1.7 μm). In fact, obvious parallel guidance entirely vanishes on the smallest periodicity. As can be seen in the data, the distribution of parallel growth tends to be very narrow, while the distribution of perpendicular growth is much wider.

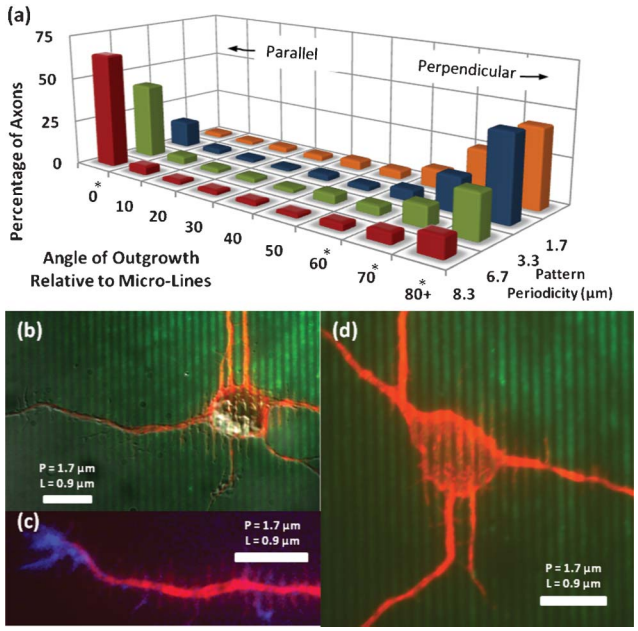

Fig. 6 Axonal Outgrowth: Varying P, Fixed L/P (a) Directional outgrowth of axons is measured and grouped into 10° bins. The transition from parallel to perpendicular guidance is seen as periodicity (P) decreases, while L/P is held at 0.5. * indicates $p < 0.01$ for a given orientation by ANOVA. (b–d) Outgrowth on P = 1.67 μm micro-lines. At this scale parallel axonal alignment is all but absent, although microtubules are still seen to align within the soma (d). Perpendicular vinculated growth is very dominant (b, c). All scale bars: 10 μm.

dendrites, were frequently aligned with the micro-lines (Fig. 3b, 4d, 6b, 6d) especially for large P and small L. For example, 90% of neurons growing parallel (within 10°) to P = 8.3 μm micro-lines had mostly parallel dendrites (92% of all dendrites) and also 90% of neurons growing perpendicular to P = 3.3 μm micro-lines had mostly parallel dendrites (74% of all dendrites). Therefore, although the change in periodicity leads to a dramatic shift in axonal guidance, dendritic guidance over the same length scale seems to rely on pattern continuity. Interestingly, dendritic outgrowth becomes more random when P = 1.7 μm, and dendrites are not observed to align with the micro-lines.

Another unusual observation that we made was that the regions of the neurons that were on the lines, either the axonal branches running parallel with the lines (Fig. 2b) or at the cell body (Fig. 3b, 4d, 6b), exhibited inverse shadow-cast circular indentations. These appeared only along the micro-lines and may represent vesicles or vacuoles inside the cells. These structures also appear to exclude microtubules within the neurons, contributing to the discontinuous nature of tubulin labeling within the axons and at the cell bodies.

Discussion

It would be difficult to over-emphasize the ease with which the methodology here employed could be widely adopted. A biology-based lab of neither engineering expertise, nor with access to any specialized fabrication facilities could quickly produce these micro-line patterns. Not only can line width, gap width, and periodicity of microlines be controlled, but simple developments of the technique yield access to a wide variety of patterns. For example, tunable-line width grids can be formed by stamping twice, with the two stampings orthogonal (see Supplementary Data†). It is trivial to vary line width and the angle of the grid. It would also be very easy to print multiple species in succession in order to create synergistic of competitive guidance cues. Either by printing a repulsive compound or by employing a two-step stamping technique, it is possible to create cell-permissive micro-island arrays. These arrays would be variable in size, spacing and aspect ratio. While this is all possible using traditional micro-stamping techniques, each new pattern would require a new master stamp, requiring time and expense. Moreover, the high resolution demonstrated in this work would require a mask which would be more expensive than low-resolution masks. Other high-resolution patterning techniques could also produce these patterns, but only with tedium and expense.

Systematic control of pattern geometry, particularly at the length scales studied in this work, has hitherto not been satisfactorily demonstrated. Only a few studies have focused on repetitive micropatterns approaching this length scale, and most of those focus on other aspects such as gradient generation,[26,27] while ignoring possibly confounding effects of geometric variability.

Axon outgrowth is an excellent study candidate on these patterns for several reasons. Perhaps most importantly, the scale of patterning achieved here is one which reflects the typical scale of axons and growth cones, making neuronal behavior exquisitely sensitive to the scale of patterning here performed. Beyond axon outgrowth, this technique could easily be incorporated in any system where micron scale patterning is intrinsically linked to cell behavior. Possible biological assays include stem cell differentiation, cancer and other cell migration, or neuron/glia co-culture. Neurobiological assays, such as a turning assay (see Supplemental Data†) or a branching assay would benefit from precise spatial control of the studied behavior. Furthermore, this microstamping could be combined with mechanical stimuli, such as surface topography or substrate elasticity, or with diffusive chemical stimuli, by incorporating this system into a micro-fluidic device. All such factors are known to affect cell behavior. The ease of the microstamping enhances the ability to study these factors in combination.

The deviation of the results here from the results published by Clark *et al.*[12] is highly significant. Their seminal paper concludes that as the period of printed micro-lines of laminin decreases, axon growth direction becomes increasingly random. When 2 μm lines are separated by 2 μm gaps, they observed nearly entirely random outgrowth. Some differences in methodology require attention. Clark and colleagues used chick embryonic 'brain' neurons, grown on a laminin patterned quartz substrate, as compared to mouse embryonic cortical neurons, grown on poly-lysine patterned PDMS used in this study. Perhaps more subtly, Clark and colleagues

measured orientation with only two possibilities, aligned or not. If a transition toward perpendicular alignment were beginning, but not completed, it may have been misjudged as random, though this runs contrary to the raw data presented. Whatever the cause, whether in neuron type, substrate, patterned compound, or otherwise, further investigation is warranted.

The unique morphology of the vinculated growth is perhaps one of the most salient details in this work. Whether the orthogonal filopodia-like structures along the axon have a causative or merely associative relationship with perpendicular guidance remains to be determined. When measuring growth cone dynamics, it was found[28] that dynamic microtubules were present in greater quantity on the sides rather than the leading edge of growth cones, likely due to decoupling from actin retrograde flow. Similar dynamic activity would be intriguing to explore on the micro-line substrates. In any case, it appears that expansive restructuring of the cytoskeleton is occurring. This is observed in both the extending axons and also the soma, where periodic spatial variability in concentrations of microtubules is observed. Somatic cytoskeletal restructuring cannot be assumed to be the only cause which initiates perpendicular axonal outgrowth, however, as quite frequently perpendicularly guided axons were seen originating from what were initially parallel-guided neurites. It is also significant that perpendicular guidance begins at a pattern scale consistent with the size of a growth cone. Future directions of this work include a full characterization and quantification of the sub-cellular components of the vinculated growth.

The remarkable shift in axonal guidance from parallel to perpendicular relative to the micro-lines is reminiscent of results published concerning axonal guidance of hippocampal neurons on micro-topography. Rajnicek and colleagues showed that topographies consisting of a series of grooves in quartz could elicit perpendicular guidance responses.[16] In an accompanying paper which explored guidance mechanisms, perpendicular growth exhibiting orthogonal filopodial extensions was reported,[29] much like the vinculated growth described here. Gomez and colleagues studied hippocampal neurons on micro-topography, instead using PDMS as the substrate, and observed similar perpendicular guidance.[17] In both of these efforts a relatively rigid, topographical surface was created, coated, and then cultured with cells. The current work differs in that the initial surface is smooth, and any topography created is by the coating of poly-lysine alone. Though it remains undetermined, it seems likely that the results seen in this work are not caused primarily by incidental topography. Furthermore, it is possible that elsewhere witnessed perpendicular axonal guidance on topographically modified surfaces is not due to the actual 3-D topography, but rather to the 2-D geometric surface patterning of available adhesive surfaces, *i.e.* the surface of successive adhesive ridge tops could function much like the patterned micro-line surface in this work. Regardless, more investigation is warranted to identify the mechanisms of axonal guidance resulting from competitive and cooperative combinations of adhesion and topography.

Inevitably it must be questioned whether this perpendicular guidance is necessary for *in vivo* development, or simply the result of experimental design. In support of the former possibility, it has been reported[30] that pioneering axons in the rat corticospinal tract are found to grow perpendicular to aligned astroglial cells.

Conclusions

Poly-lysine micro-lines of sub-cellular dimensions were patterned using a non-traditional micro-stamping technique. This technique enables control over patterned line width, and patterns at a scale and over an area which is difficult to achieve using more common methods. Moreover, this method is simple and inexpensive.

Cortical neurons grown on these adhesive micro-lines were shown to be strongly guided in their axonal orientation. Lines of larger periodicity reliably produced parallel axonal outgrowth, while lines of smaller periodicity induced perpendicular outgrowth. It was shown that periodicity, not line width or gap width independently, was the critical dimension that effected a transition from parallel to perpendicular axonal guidance.

Perpendicular axonal outgrowth was especially distinctive in its morphology. Growth exhibiting periodic filopodial extensions and nascent branches, oriented perpendicular to the growing axon, or parallel to the traversed micro-lines, was frequently observed. This vinculated growth occurred along axons growing perpendicular to micro-lines of all dimensions, even on micro-lines where parallel growth was favored.

References

1 C. E. Schmidt and J. B. Leach, *Annu. Rev. Biomed. Eng.*, 2003, **5**, 293–347.
2 K. Bossers, G. Meerhoff, R. Balesar, J. W. Van Dongen, C. G. Kruse, D. F. Swaab and J. Verhaagen, *Brain Pathol.*, 2009, **19**, 91–107.
3 D. A. Heller, V. Garga, K. J. Kelleher, T. C. Lee, S. Mahbubani, L. A. Sigworth, T. R. Lee and M. A. Rea, *Biomaterials*, 2005, **26**, 883–889.
4 B. C. Wheeler and G. J. Brewer, *Proc. IEEE*, 2010, **98**, 398–406.
5 M. O'Donnell, R. K. Chance and G. J. Bashaw, *Annu. Rev. Neurosci.*, 2009, **32**, 383–412.
6 D. Koch, W. J. Rosoff, J. Jiang, H. M. Geller and J. S. Urbach, *Biophys. J.*, 2012, **102**, 452–460.
7 D. Falconnet, G. Csucs, H. Michelle Grandin and M. Textor, *Biomaterials*, 2006, **27**, 3044–3063.
8 H. C. Tai and H. M. Buettner, *Biotechnol. Prog.*, 1998, **14**, 364–370.
9 M. Song and K. E. Uhrich, *Ann. Biomed. Eng.*, 2006, **35**, 1812–1820.

10 L. Kam, W. Shain, J. N. Turner and R. Bizios, *Biomaterials*, 2001, **22**, 1049–1054.
11 K. G. Sharp, G. S. Blackman, N. J. Glassmaker, A. Jagota and C. Y. Hui, *Langmuir*, 2004, **20**, 6430–6438.
12 P. Clark, S. Britland and P. Connolly, *J. Cell. Sci.*, 1993, **50**, 385–397.
13 X. Younan, J. Tien and G. M. Whitesides, *Langmuir*, 1996, **12**, 4033–4038.
14 C. Y. Hui, A. Jagota, Y. Y. Lin and E. J. Kramer, *Langmuir*, 2002, **18**, 1394–1407.
15 Y. Xia and G. Whitesides, *Langmuir*, 1997, **13**, 2059–2067.
16 A. M. Rajnicek, S. Britland and C. D. McCaig, *J. Cell. Sci.*, 1997, **110**, 2905–2913.
17 N. Gomez, Y. Lu, S. Chen and C. E. Schmidt, *Biomaterials*, 2007, **28**, 271–284.
18 W. K. Cho, K. Kang, G. Kang, M. J. Jang, Y. Nam and I. S. Choi, *Angew. Chem., Int. Ed.*, 2010, **49**, 10114–10118.
19 C. Viesselmann, J. Ballweg, D. Lumbard and E. W. Dent, *J. Vis. Exp.*, 2011, **pii**, 2373.
20 E. W. Dent and K. Kalil, *J. Neurosci.*, 2001, **21**, 9757–9769.
21 S. M. Sarkar, P. D. Rourke, T. A. Desai and J. Y. Wong, *Acta Biomater.*, 2005, **1**, 93–100.
22 A. W. Feinberg, W. R. Wilkerson, C. A. Seegert, A. L. Gibson, L. Hoipkemeier-Wilson and A. B. Brennan, *J. Biomed. Mater. Res., Part A*, 2008, **86A**, 522–534.
23 D. Fuard, T. Tzvetkova-Chevolleau, S. Decossas, P. Tracqui and P. Schiavone, *Microelectron. Eng.*, 2008, **85**, 1289–1293.
24 M. N. De Silva, R. Desai and D. J. Odde, *Biomed. Microdevices*, 2004, **6**, 219–222.
25 E. W. Dent, J. L. Callaway, G. Szebenyi, P. W. Baas and K. Kalil, *J. Neurosci.*, 1999, **19**, 8894–8908.
26 A. C. von Philipsborn, S. Lang, J. Loeschinger, A. Bernard, C. David, D. Lehnert, F. Bonhoeffer and M. Bastmeyer, *Development*, 2006, **133**, 2487–2495.
27 R. Fricke, P. Zentis, L. Rajappa, B. Hofmann, M. Banzet, A. Offenhäusser and S. Meffert, *Biomaterials*, 2011, **8**, 2070–2076.
28 A. C. Lee and D. M. Suter, *Dev. Neurobiol.*, 2008, **68**, 1363–1377.
29 A. Rajnicek and C. McCaig, *J. Cell. Sci.*, 1997, **110**, 2915–2924.
30 E. A. J. Joosten and D. P. R. Bär, *J. Anat.*, 1999, **194**, 15–32.